Peer-reviewed version available at Sensors 2018, 19, 12; doi:10.3390/s19010012

Article

Temperature measurement of fluids flow by using a focusing schlieren method

A. Martínez-González[2, 3, *], D. Moreno-Hernández[1, *], J. A. Guerrero-Viramontes[3], M. León-Rodríguez[4], J. C. I. Zamarripa-Ramírez[1] and C. Carrillo-Delgado[2].

[1] Centro de Investigaciones en Óptica A.C., Loma del Bosque 115, Lomas del Campestre, CP 37150, León, Guanajuato, México.
[2] Depto. de Ingeniería Robótica, Universidad Politécnica del Bicentenario, Carr. Silao - Romita Km 2, San Juan de los Duran, C.P. 36283, Silao, Guanajuato, México.
[3] TecNM/Instituto Tecnológico de Aguascalientes, Adolfo López Mateos 1801., Aguascalientes AGS. 20256, México.
[4] Universidad Politécnica de Guanajuato, Av. Universidad sur 1001, C.P. 38496 Cortázar, Guanajuato, México.
* Correspondence: amartinezg@upbicentenario.edu.mx; dmh@cio.mx

Abstract: In this work, we propose a method to measure planar temperature fields of fluids flow. We used a focusing schlieren technique together with a calibration procedure to fulfill such purpose. The focusing schlieren technique uses an off-axis circular illumination to reduce the depth of focus of the optical system. The calibration procedure is based on the relation of the intensity level of each pixel of a focused schlieren image to the corresponding cutoff grid position measured at the exit focal plane of the schlieren lens. The method is applied to measure planar temperature fields of the hot air issuing from a 10 mm diameter nozzle of a commercial Hot Air Gun Soldering Station Welding. Our tests are carried out at different temperature values and different planes along the radial position of the nozzle of the Hot Air Gun Soldering Station Welding. The temperature values obtained experimentally are in agreed with those obtained with a thermocouple.

Keywords: focusing schlieren, temperature, measurements

1. Introduction

The interest of temperature measurement is present in several branches of science. The optical full field techniques are preferred to fulfill such an important task. The most common optical techniques used to measure temperature in transparent media are: interferometry, holography, laser speckle photography, and the schlieren techniques [1].

The schlieren technique is one of the most successful optical method used to visualize fluids flow because of its relatively easy implementation, low cost, use of conventional light sources, and its high and variable sensitivity [2, 3]. This technique has been improved to face different kinds of problems in different fields of knowledge [4-24]. Although the schlieren technique was primarily conceived as a visualization method, it has also been used to obtain quantitative temperature data in fluids flow [8-16]. Consequently, some of the approaches proposed to accomplish such a purpose are: color schlieren [10-12], background oriented schlieren [13,14] and calibration schlieren [15,16]. In addition, the technique has been extended to measure simultaneously temperature and velocity in fluids flow [19-22].

Peer-reviewed version available at Sensors 2018, 19, 12; doi:10.3390/s19010012

One deficiency of the schlieren technique is that it provides information that is integrated along the optical path. Therefore, such information is not exact for a three-dimensional temperature field when a standard two-dimensional analysis technique is applied. The main reason is that the schlieren methods average the refractive index variations along the width of the object under analysis making local temperature measurement difficult. Not so with a focusing imaging technique in which it is possible to visualize only the refractive index disturbances in a limited volume along the optical path. Thereby, focusing schlieren systems is useful to explore a three-dimensional refractive field by incrementally visualizing individual planes along the optical path but perpendicular to it.

The focusing schlieren methods allow achieving a narrow depth of focus useful to obtain planar temperature measurements in three-dimensional fluids flow. The focusing image techniques for studying fluids flow have been previously explored for several authors [23-29]. Some authors proposed a focused schlieren system by transforming a classical schlieren set-up to obtain quasi-planar measurements [23-25]. Other variants of the focused schlieren system were described in [26, 27]. However, these systems had a limited field of view imposed by the optical components used on the experimentation. In another approach, a light source that illuminates a source grid and a Fresnel lens was used to improve the method [28, 29]. In a recently research, a structured light-field focusing technique was proposed to visualize fluids flow [30]. This approach stems for using light-field physics and multiple light sources to generate two-dimensional planar focused images. Also, this approach is simple to implement, flexible to applied to various fluids flow conditions, and can be aligned easier. Indeed, most of the studies about focusing schlieren techniques have been used to visualize the behavior of fluids flow under different circumstances [31, 32]. Very few of these optical arrangements have been used to quantify a variable of a fluid flow [33]. In this way, in the present work, we propose an approach in which we measure temperature fields on a narrow region in fluids flow.

The proposed technique to measure planar temperature fields is based in a relation between the intensity levels of each pixel of a focused schlieren image to the corresponding cutoff grid position measured at the exit focal plane of the optical system. The focusing schlieren images are obtained using a focusing schlieren optical system based on an off-axis circular illumination. The kind of illumination used in this work permit us to generate an expanded synthetic aperture that improves the depth of focus of the optical system. This focusing effect neglect out-of-focus features, so that region of interest can be enhanced. By this technique, we have been able to measure temperature fields in different planes along the radial position of the nozzle of a commercial Hot Air Gun Soldering Station Welding.

2. Theoretical development

It is well known that when a light ray passes through an inhomogeneous medium it suffers a deviation in its trajectory by a certain angle [2-3, 34]. This angle depends on the refractive index and thickness of the medium under test. The angle of the ray deviation can be represented as:

$$\varepsilon_{\xi} = \int_{\zeta_1}^{\zeta_2} \frac{\partial n}{\partial \xi} dz, \tag{1}$$

Peer-reviewed version available at Sensors 2018, 19, 12; doi:10.3390/s19010012

where $n = n(x, y, z)$ is the refractive index of the medium, and ξ can be "x" or "y", depending on the direction in which the cutoff grid blocks out the light. In this work the analysis is done for the x-direction.

By combining the Gladstone-Dale's equation, $(n\text{-}1) = K\rho$, and equation (1), we get the following equation:

$$\rho_x = \frac{\partial \rho}{\partial x} = \frac{\delta x}{f \mathrm{hK}}, \tag{2}$$

where ρ is the gas density, h is the thickness (region of interest in focus) of the inhomogeneous medium under test in the direction of ray propagation, f is the focal lens of the schlieren lens and K is the Gladstone-Dale's constant. The Gladstone-Dale's constant is a function of both; the wavelength of the light source and the physical properties of the gas. In the present study, its value was taken as 2.271×10-4 m3/kg, for an air temperature at 293 K and a wavelength of 530 nm [2].

For an ideal gas at constant pressure, the temperature can be found from the Gladstone-Dale's equation, which reduces to the following form [35]:

$$T = \frac{\rho_o}{\rho} T_o = \frac{n_o - 1}{n - 1} T_o. \tag{3}$$

In equation (3), n_o and ρ_o are the refractive index and density at reference temperature T_o, respectively, and T is the temperature of interest. In this way, the aim in our approach is to determine the value δx of equation (2) by a calibration procedure [16, 18]. In the next section, we give a briefly explanation of the method used to measure temperature fields by using a focusing schlieren optical system.

3. The focusing schlieren method base on an off-axis circular illumination

In figure 1 is shown the focusing schlieren system used in this work [30]. The optical system contains a source grid (F-G), a schlieren lens (D), a cutoff grid (C) and a digital camera (A-B). The sample test (E) is placed between the source grid and the schlieren lens. The source grid is a two-dimensional discrete light source array. It was assembled by using a green light circular lamp (G) of diameter 180 mm and a light aperture (F). The circular lamp has a power of 18 W and a luminous flux of 1200 lm. The light aperture is made of a 0.5 mm thick black plastic sheet and is stuck on the surface of the lamp. The light aperture contains 12 circular orifice of diameter 3 mm positioned on a circular array pattern. Each hole is off-axis from the centre of the circular lamp a distance of 60 mm. This array pattern configuration allows us to form an expanded synthetic aperture in order to reduce the Depth Of Focus (*DOF*) of the optical system. Also, there is an orifice of diameter 3 mm at the center of the light aperture used to test the *DOF* of the optical system illuminated with a source located on the optical axis.

In the system presented in this study, the schlieren lens ($f_\#$ = 2.3) has a fixed focal length and a diameter of 215 mm and 90 mm respectively. The cutoff grid was made of the same black plastic sheet used to make the light aperture. The cutoff grid is scaled from the light aperture to a magnification of 0.641 given by the schlieren lens. The orifices of the cutoff grid are square of side 1 mm and are arrange in a circular pattern also. The cutoff grid was placed to emphasize density gradients in the stream-wise direction of the fluid flow. The object at the test area was imaged on

the digital camera (A) by using a lens (B- $f_{\#}$ = 1.7) with a fixed focal length of 128 mm and a diameter of 75 mm. When the optical system is aligned, the source grid at D_o is an optical conjugate with the cutoff grid at D_i. Also, the object plane at d_o is an optical conjugate with the image position at d_i. The positions of the conjugate planes can be determined by the thin lens equation [36].

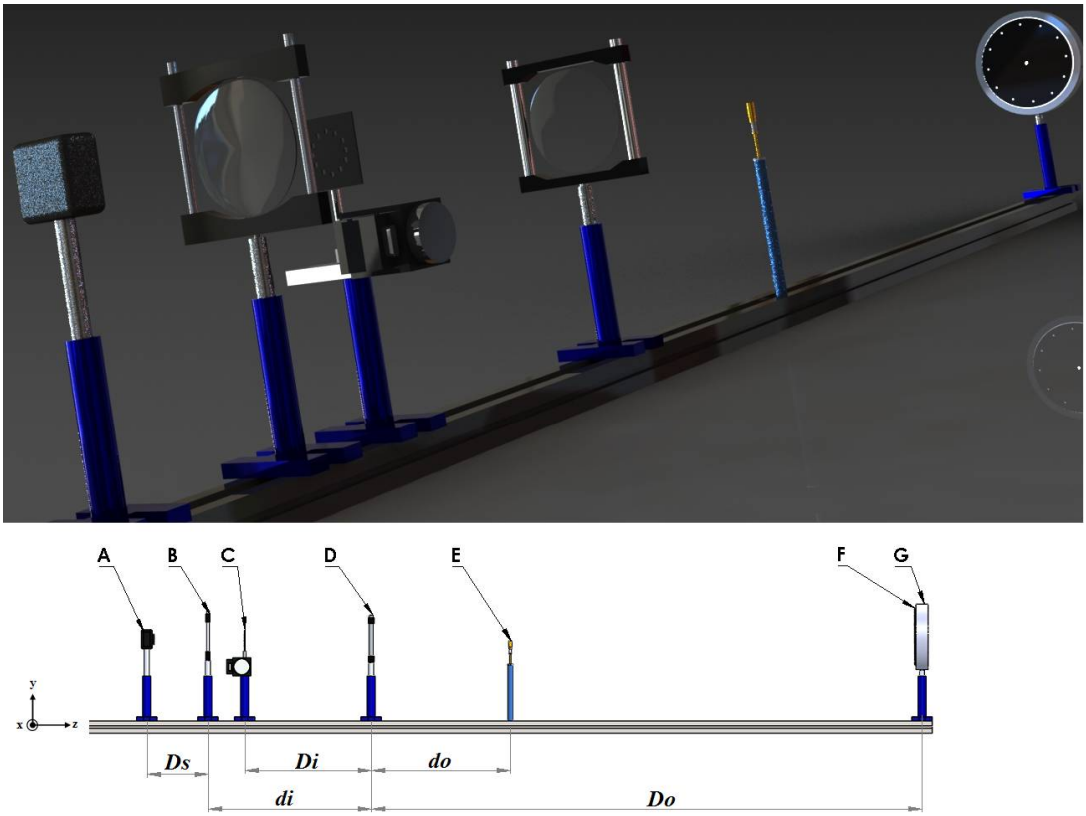

Figure 1. A focusing schlieren system based on an off-axis circular illumination.

The optical elements used in our set-up allow us to calculate the parameters needed to test the performance of the method. Our system allows us having a Field Of View (*FOV*) of 17.4×9.2 mm. The DOF of the focusing-schlieren system for one source [30] is written as follows

$$DOF = \frac{2d_o f^2 c f_{\#}(d_o - f)}{f^4 - c^2 f_{\#}^2 (d_o - f)^2} \tag{4}$$

where c is the confusion circle, $f_{\#}=f/d$, and f and d are the focal distance and diameter of the schlieren lens respectively. The modified f - number for an off axis source can be expressed as:

$$f_{\#} = \frac{f}{d + (2 \cdot OS)} \tag{5}$$

where *OS* is the off axis distance from the axis of the optical system to a source of the source grid. The effective *DOF* of the system depends of the number of sources. Then, a lineal equation expressing this relation can be written as [29],

$$DOF_S \approx \frac{DOF}{Ns} \tag{6}$$

Peer-reviewed version available at Sensors 2018, 19, 12; doi:10.3390/s19010012

where *Ns* is the number of sources. In our approach, the calculations of the *DOF* were done for three cases, i.e, one source, and six and twelve sources. The number of sources needed for the experiment was realized by maintaining uncovers one, six and twelve orifices of the source grid. The *DOF* for the one source case was estimated by maintaining uncover only the orifice located at the centre of light aperture.

From equations 4-7, we can infer that to have high sensitivity and narrow *DOF* imaging system requires a large f and small $f_{\#}$ of the schlieren lens. Figure 2 shows the behavior of the *DOF* in function of the object plane position and the number of sources. Note that the *DOF* is smaller as the object plane approaches to focus plane and because of the number of sources. For these calculations was used a circle of confusion of c=2 mm [29]. Note that these values are theoretical, determined by ideal equations and some discrepancies can be obtained in the experimental results.

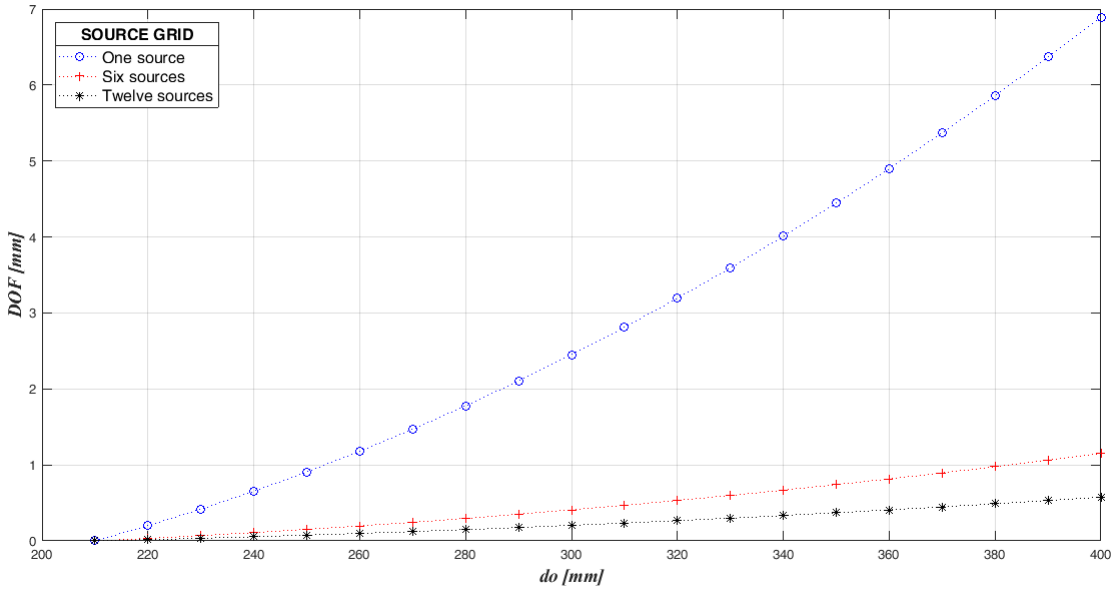

Figure 2. Performance of the focusing schlieren system used in this work

The performance of our system is tested experimentally by imaging a 0.6 mm dot of a calibration slide. The calibration dot is useful to accurate characterization of the focusing effect. Figure 3 shows the *DOF* effect of a dot of a calibration slide by using one, six and twelve light sources. The calibration slide was fixed to a mount for a proper displacement. For a better comparison, a small section of the entire image was selected. In the figure 3, the up, middle and down dot images correspond to the *DOF* test using one, six and twelve light sources respectively. In our analysis "z" is measured along the optical axis and the slide is moving away from the camera. The focusing schlieren images were obtained at various calibration slide positions. We can observe that in the first case (one light source), the shape of the dot images at z=0.0, 0.5 mm, 1.0 mm, and 2.0 mm appear very well defined. Indeed, it is very difficult to find differences between the four images. The experimental *DOF* calculated for this case was of ~4.6 mm. In the two remaining cases, the shape of the dot was clearly visible in the plane of best focus (0 mm) and barely blurred at z=0.5 mm. On the other hand, the shape of the dot was blurred at the planes z= 1.0 mm and 2.0 mm. In these two last cases, the value of the experimental *DOF* obtained was of ~0.8 mm and ~0.4 mm for six and twelve sources respectively.

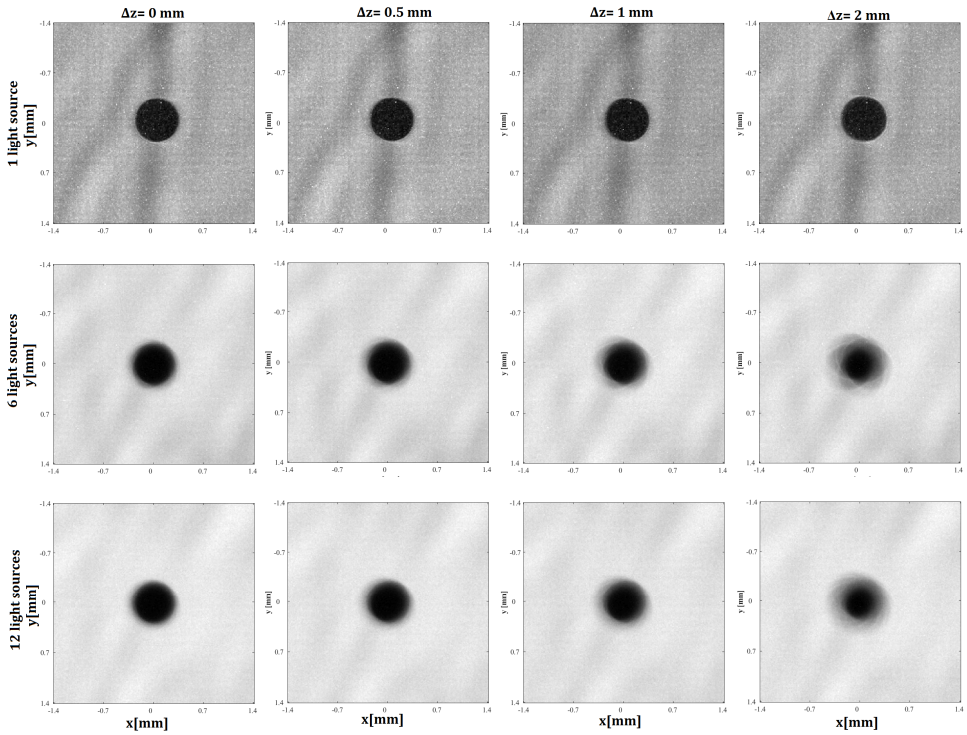

157 **Figure 3.** Focusing Focusing effect of a dot of a calibration slide. Top images: one source. Middle images: six
158 sources. Bottom images: twelve sources. The images are registered moving the calibration slide away from the
159 camera.

160 The experiments realized in this section were used to test the performance of the optical system
161 used in this work by utilizing specific characteristics of the optical components. In this way, the
162 system with twelve light sources offers us the narrower *DOF*, and is used to measure planar
163 temperature fields of a commercial Hot Air Gun Soldering Station Welding.

164 **4. Method to measure temperature in fluids flow**

165 The basic idea behind the procedure to measure temperature in fluids flow is to relate the
166 intensity level of each pixel of a focused schlieren image to the corresponding cutoff grid position at
167 the exit focal plane of the schlieren lens [16,18]. Each light source of the source grid is focused at the
168 image plane of the schlieren lens. It is in this point where the cutoff grid is placed. Each individual
169 image formed for each source overlap on the image plane creating a sharp focused image. The
170 transverse position of the cutoff grid may cover the conditions from no cutoff of light (maximum
171 intensity) to full cutoff of light (minimum intensity). This procedure allows us to obtain a calibration
172 curve which is subtracted to the focused schlieren image obtained when the cutoff grid is at the
173 reference position (I_o). The reference position represents the condition when the cutoff grid is in its
174 reference position, which in this analysis corresponds to a position such that the light intensity at the
175 observation plane represents an intermediate intensity value between cutoff and no cutoff, i.e., when
176 the intensity value is about 50% of the light observed for the condition of no cutoff.
177 These calibration curves represent intensity deviations versus cutoff grid position (δx). A typical
178 calibration curve is shown in figure 4. This is equivalent to do an image mathematical subtraction,
179 i.e., the intensity of a focused schlieren image in presence of flow (I_f) from a focused schlieren image
180 with no flow or with undisturbed conditions (I_o). When the transverse cutoff grid position, δx, from

Peer-reviewed version available at Sensors 2018, 19, 12; doi:10.3390/s19010012

the calibration curves has been assigned to its corresponding intensity value for all pixels of a focused schlieren image, in presence of flow, the ρ_x value can be determined via equation (2). The density value can be stated as [3]:

$$\rho(x) = \rho_0 + \frac{1}{f_2 \mathrm{hK}} \int_{\zeta_1}^{\zeta_2} \delta x dx. \tag{7}$$

The trapezoidal numerical integration algorithm is used to integrate equation (7). In references [16, 18] is included a description of the procedure used in this work to determine temperature measurements.

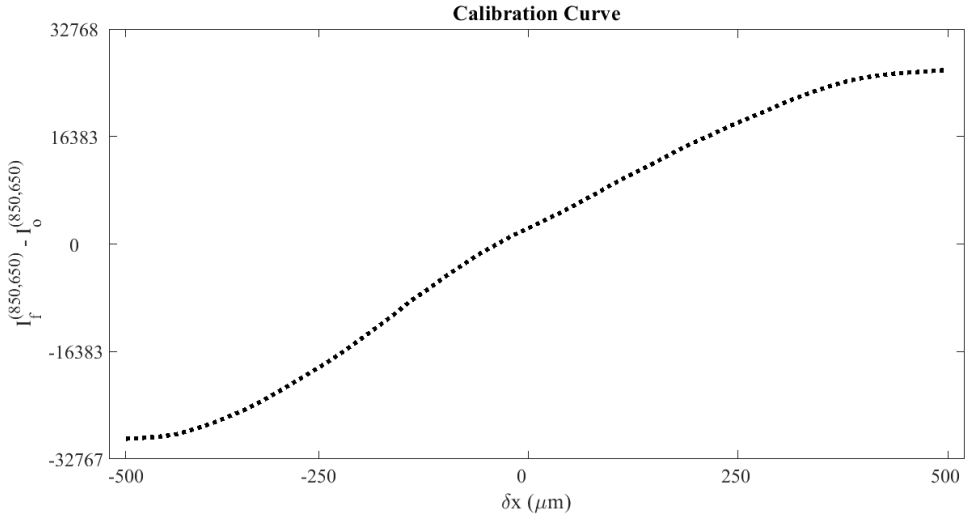

Figure 4. A typical calibration curve of a pixel.

5. Experiment

This experiment is aimed to measure temperature fields of the hot air issuing from a 10 mm diameter nozzle of a commercial Hot Air Gun Soldering Station Welding (HAGSSW). The Hot air gun soldering station welding is a programmable digital display iron soldering. The programmable soldering allows us inducing air temperatures from 100 °C up to 600 °C. In our experiments the hot air soldering was set to temperature values of 200 °C and 400 °C. These values were corroborated by utilizing a K-type thermocouple probe provided by Fluke. The thermocouple was positioned near the exit of the nozzle of the soldering station.

A focusing schlieren system is used in this research. The technical characteristics of the optical setup were introduced in section 3. Figure 1 shows a schematic of the experimental arrange. The nozzle of the hot air soldering station is positioned horizontally on an optical table. The stream-wise direction of the fluid flow is at y-direction, and the cutoff grid is moved perpendicular to this direction. The temperature measurements of the hot air issuing from the nozzle were done in three planes, i.e., $z = 0, \pm 5$ mm.

The focusing schlieren images are acquired with a Lumenera color digital camera, which can provide 170 frames per second at a spatial resolution of 2048 × 1088 pixels, and it has a pixel size of 5.5 μm. These images are stored in BMP format and digitized by a 16-bit color level frame grabber. The camera is driven by software that lets us take either a single frame or a set of them. In our experiment only the images of the green color-channel were used. The selected spatial resolution of the camera allows us to capture the main characteristics of the fluid flow under study.

The first step of the experiment consists in recording focusing schlieren images with no flow for several transverse positions of the cutoff grid covering the conditions of no cutoff of light to full cutoff of light. These images are used for calibration purposes as it was briefly explained in section 4. After that, we acquired a total of 100 focused schlieren images with flow for each case under analysis. All measurements were done at a room temperature of 23 ºC.

6. Data analysis

In order to show the viability of the method, we determine the temperature fields from the experimental data outlined in section 5 of the hot air issuing from the nozzle of the HAGSSW.

6.1. Temperature data analysis

The value of ρ_x is determined by using the calibration procedure explained in section 4. Integration of this quantity is required to obtain the value of ρ as it is shown in equation (7). The resulting density values are substituted in equation (3) in order to obtain the temperature of interest.

In figure 5, a flow chart of the procedure is depicted. To obtain calibrations curves for each pixel, the cutoff grid is laterally displaced from -500 µm to 500 µm with a step size of 20 µm, and at each cutoff grid position, a focused schlieren image is recorded. Figure 6 shows calibration images for different cutoff grid positions. All the focused schlieren images are subtracted from the image with the cutoff grid in its reference position (upper path in the flow chart). In the flow chart and figure 6, the focused schlieren image with the cutoff grid in its reference position is indicated by a red square. On the lower path of the flow chart, a particular focused schlieren image in presence of flow, with the cutoff grid at its reference position, is shown. This image is subtracted from a focused schlieren image with no flow and the cutoff grid at its reference position. Therefore, the light deviation intensity for each pixel is directly related to its corresponding calibration curve. In this way, intensity deviation values of all pixels of each image are converted to cutoff grid displacement.

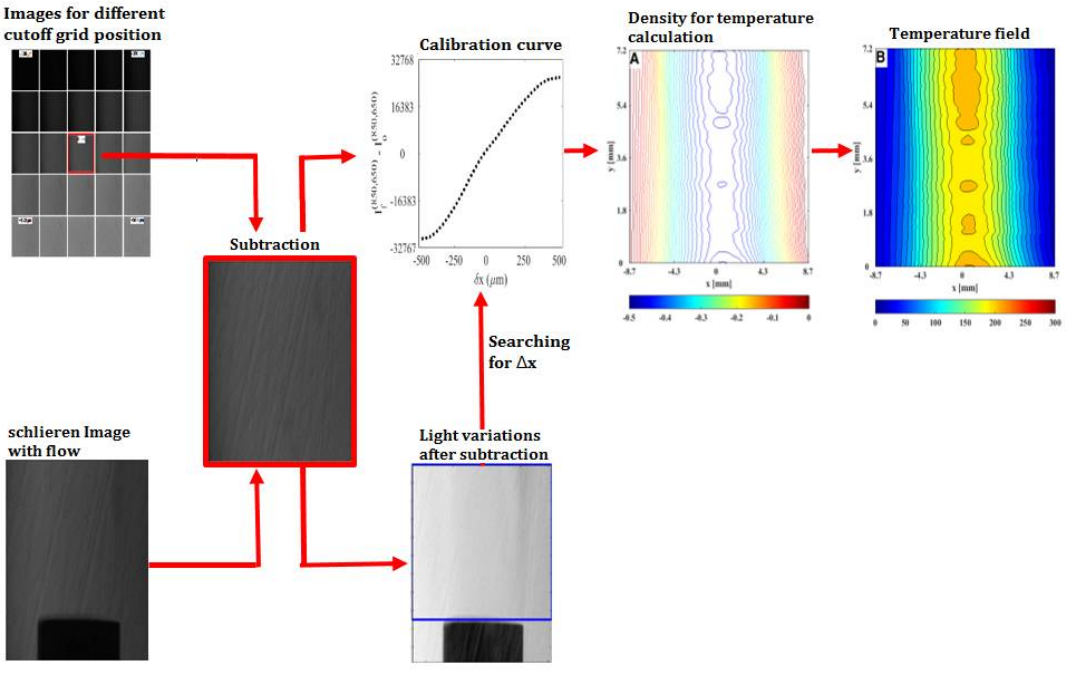

Figure 5. The flow chart for temperature measurements of fluids flow by using a focusing schlieren system.

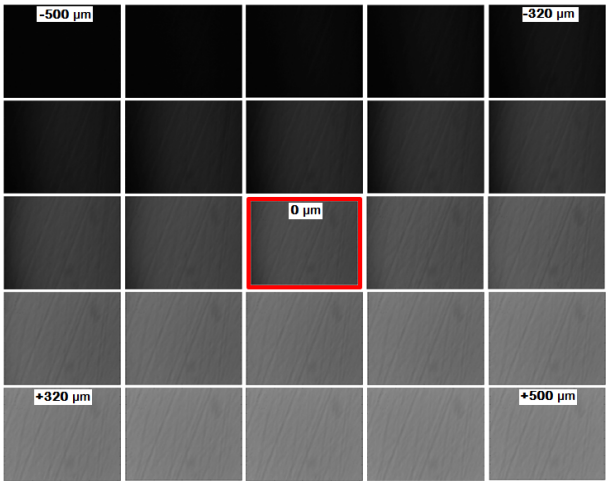

Figure 6. Focusing schlieren images for different cutoff grid positions for calibration purposes.

Figure 7 and 8 show instantaneous focused schlieren images after convert to δx displacement and its corresponding temperature fields of the hot air issuing from the nozzle of the HAGSSW. It is clear that in the images there are some imperfections caused by the schlieren lens. However, this effect does not affect the calculation of the temperature. Also, notice the differences of the temperature fields at symmetrical planes, i.e, z=±5 mm. These discrepancies are due to non-uniformity in the fluid flow. Indeed, the optical system presented in this study is useful for characterizing the operation of the commercial HAGSSW and for non-symmetrical fluids flow.

We found that the temperature near the exit of the nozzle of the HAGSSW is consistent with the temperature values set at the programmable HAGSSW. In figure 9, we show average temperature fields for the two different temperature values under analysis. We used 100 focused schlieren images to obtain the temperature average values. These temperature values were corroborated by a thermocouple measurement located near the exit and at the center of the nozzle of the HAGSSW as it has been indicated on the figure 9. The relative error between both measurements for each case is of ~7.8% and ~9.0%. These differences in measurements can be due to several factors such as fluid flow fluctuations, lens aberrations and errors inherent of the measurement process.

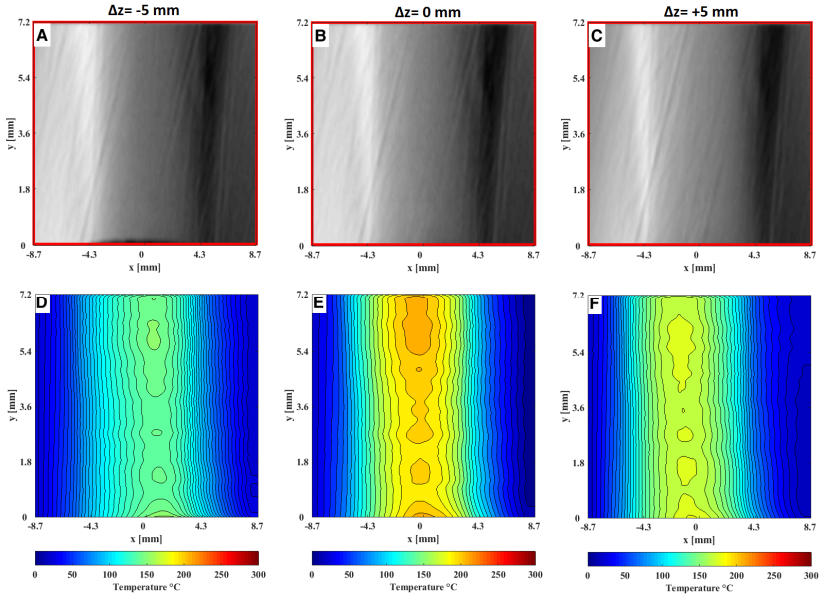

Peer-reviewed version available at Sensors 2018, 19, 12; doi:10.3390/s19010012

Figure 7. Instantaneous focusing schlieren images of the hot air issuing from the nozzle of the HAGSSW at 200 °C. A, B and C are the focusing schlieren images after convert each intensity level of pixels to cutoff grid displacements (δx) at planes z= -5 mm, z=0 mm , z=5 mm respectively. D, E and F are the corresponding temperature field at planes z= -5 mm, z=0 mm , z=5 mm respectively.

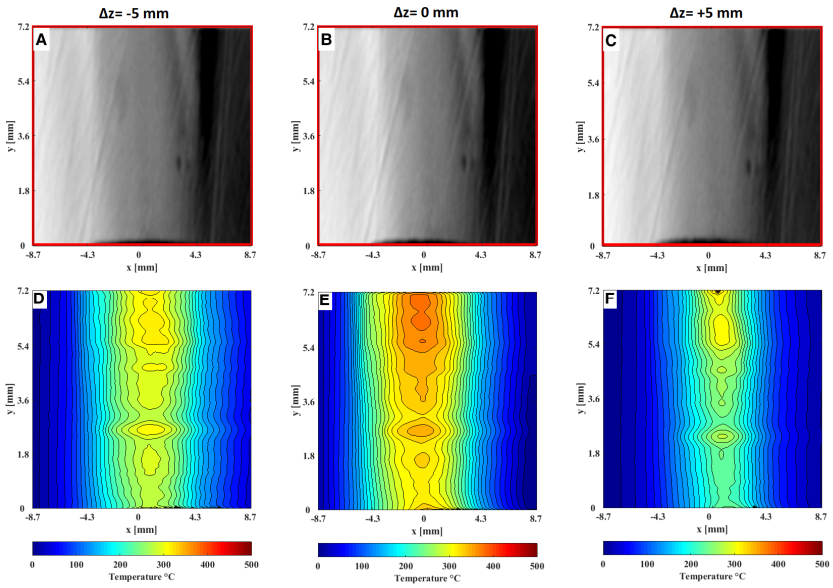

Figure 8. Instantaneous focusing schlieren images of the hot air issuing from the nozzle of the HAGSSW at 400 °C. A, B and C are the focusing schlieren images after convert each intensity level of pixels to cutoff grid displacements (δx) at planes z= -5 mm, z=0 mm , z=5 mm respectively. D, E and F are the corresponding temperature field at planes z= -5 mm, z=0 mm , z=5 mm respectively.

The approach presented in this work allows us to obtain a minimum local temperature value of ~23 °C. On the other hand, we used the experimental data obtained in this study to calculate standard deviation for each case under study. The uncertainty was computed for measurements near and centre of the exit of the nozzle of the soldering station, i.e., at z=0. We select this position since we expect to have lower fluid flow fluctuations. We obtained uncertainty values of 2.5 °C and 3.7 °C of the hot air issuing of the HAGSSW nozzle set at temperature values of 200 °C and 400 °C respectively.

The optical system presented in this study offer some specific characteristics that limit the range of temperatures to be measured and the kind of object to be analyzed. In order to change the capabilities of our optical system, we may use optical components to have a wider FOV, high quality lenses to increase the accurate of temperature measurements, and high speed digital cameras to study high speed phenomena.

Peer-reviewed version available at Sensors 2018, 19, 12; doi:10.3390/s19010012

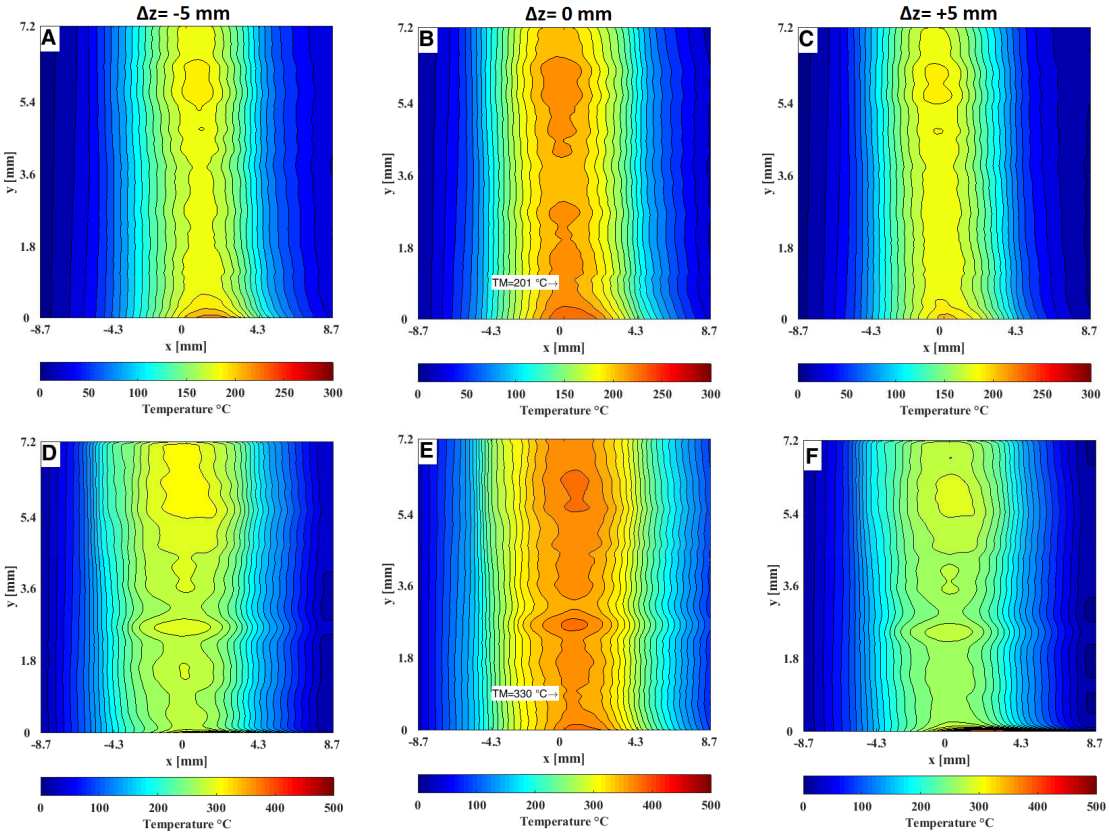

Figure 9. Average temperature fields utilizing 100 focusing schlieren images of the HAGSSW. A, B and C represent first case (200 °C) at planes z= -5 mm, z=0 mm , z=5 mm respectively. D, E and F represent second case (400 °C) at planes z= -5 mm, z=0 mm , z=5 mm respectively. TM: means, location and thermocouple measurement.

5. Conclusions

We reported planar temperature measurements of the hot air issuing from a nozzle of a Hot Air Gun Soldering Station Welding. A simple focusing schlieren system based on an off axis illumination was used for that purpose. The use of an off axis illumination allows to focus in a narrow region of the fluid flow. This focusing effect neglect out-of-focus features, so that region of interest can be enhanced. Thus, the off axis illumination used in this work permits us to generate a larger synthetic aperture than the actual aperture of the schlieren lens. Our approach allows us to obtain a narrow depth of focus of the order of ~ 0.4 mm useful to attain planar temperature measurements in fluids flow. Also, in order to measure temperature fields, the proposed method makes use of a calibration procedure that allowed us to directly convert intensity level for each pixel of a focused schlieren image into a corresponding transverse cutoff grid position. The approach proposed in this work is useful to explore a three-dimensional temperature field by incrementally visualizing individual planes along the optical path but perpendicular to it. The temperature values results are in agreed with those obtained with a thermocouple. In future work, the system will be improved by using a high-speed digital camera, high quality lenses with of different characteristics, and different kind of illumination sources. We want to develop a digital focusing schlieren system that uses larger format lenses to reach greater sensitivity and larger fields of view.

References

1. C. Tropea; A. Yarin; J Foss. Handbook of experimental fluid mechanics, Springer, Berlin, 2007; ISBN 978-3-662-49162-1
2. W. Merzkirch. Flow visualization, 2nd ed., Academic Press, Orlando, 1987; ISBN 0124913512
3. G. S. Settles. Schlieren and shadowgraph techniques, 1st ed., Springer, Berlin 2001; ISBN 978-3-642-63034-7
4. N. F. Barnes; S. L. Bellinger. Schlieren and shadowgraph equipment for air flow analysis, *J. Opt. Soc. Am.* **1945,** *35*, 497-509, https://doi.org/:10.1364/JOSA.35.000497.
5. R. A. Burton. A modified Schlieren apparatus for large areas of field, *J. Opt. Soc. Am.* **1949**, *39*, 907-908, https://doi.org/10.1364/JOSA.39.000907
6. G. Decker; R. Deutsch; W. Kies and J. Rybach. Computer-simulated Schlieren optics, *Appl. Opt.* **1985**,*24*, 823-828. https://doi.org/10.1364/AO.24.000823
7. A. Korpel; T. T. Yu; H. S. Snyder and Y. M. Chen. Diffraction-free nature of Schlieren sound-field images in isotropic media, *J. Opt. Soc. Am.* **1994,** 11, 2657-2663. https://doi.org/10.1364/JOSAA.11.002657
8. S. Stanic. Quantitative Schlieren visualization, *Appl. Opt.* **1978**, *17*, 837-842. https://doi.org/10.1364/AO.17.000837
9. R. E. Peale and P. L. Summers. Zebra schlieren optics for leak detection, *Appl. Opt.* **1996**, *35*, 4518-4521. https://doi.org/10.1364/AO.35.004518
10. A. K. Agrawal; N. K. Butuk; S. R. Gollahalli and D. Griffin. Three-dimensional rainbow Schlieren tomography of a temperature field in gas flows, *Appl. Opt.* **1998,** *37*, 479-485. https://doi.org/10.1364/AO.37.000479
11. V. P. Tregub. A color Schlieren method, *J. Opt. Technol.* **2004** ,*71*, 785-790. https://doi.org/10.1364/JOT.71.000785
12. T. Wong and A. K. Agrawal. Quantitative measurements in an unsteady flame using high-speed rainbow schlieren deflectometry, *Meas. Sci. Technol.* **2006** ,*17*, 1503–1510. https://doi.org/10.1088/0957-0233/17/6/031
13. E. M. Popova. Processing Schlieren-background patterns by constructing the direction field, *J. Opt. Technol*. **2004** , *71*, 572-574. https://doi.org/10.1364/JOT.71.000572
14. M. Raffel; H. Richard and A. G. E. A. Meier. On the applicability of background oriented optical tomography for large scale aerodynamic investigations, *Exp. Fluids.* **2000** ,*28*, 477-481. https://doi.org/10.1007/s003480050408
15. S. Garg and L. N. Cattafesta. III, Quantitative schlieren measurements of coherent structures in a cavity shear layer, *Exp. Fluids* **2001** ,*30*, 123–134. https://doi.org/10.1007/s003480000147
16. C. Alvarez-Herrera; D. Moreno-Hernández; B. BarrientosGarcía and J. A. Guerrero-Viramontes. Temperature measurement of air convection using a schlieren system, *Opt. Laser Technol*. **2009** ,*41*, 233–240. https://doi.org/10.1016/j.optlastec.2008.07.004
17. S. B. Dalziel; M. Carr; J. K. Sveen and P. A. Davies. Simultaneous synthetic schlieren and PIV measurements for internal solitary waves, *Meas. Sci. Technol.* **2007** ,*18*, 533–547. https://doi.org/10.1088/0957-0233/18/3/001
18. A. Martínez-González; J. A. Guerrero-Viramontes and D. Moreno Hernández. Temperature and velocity measurement fields of fluids using a schlieren system, *Appl. Opt.* **2012** ,*51* (16), 3519-3525. https://doi.org/10.1364/AO.51.003519
19. A. Martínez-González; D. Moreno Hernández and J. A. Guerrero-Viramontes. Measurement of temperature and velocity fields in a convective fluid flow in air using schlieren images, *Appl. Opt*. **2013** ,*52 (22)*, 5562-5569. https://doi.org/10.1364/AO.52.005562
20. L. Prevosto; G. Artana; B. Mancinelli and H. Kelly. Schlieren technique applied to the arc temperature measurement in a high energy density cutting torch, *J. Appl. Phys.* **2010** ,*107 (22).* https://doi.org/10.1063/1.3291099
21. Jacob C. Kaessinger; Kramer C. Kors; Jordan S. Lum; Heather E. Dillon and Shannon K. Mayer. Utilizing Schlieren Imaging to Visualize Heat Transfer Studies , ASME 2014 International Mechanical Engineering Congress and Exposition, Volume 5, Montreal, Quebec, Canada, November 14–20, (2014).
22. P. Aleiferis; A. Charalambides; Y. Hardalupas; N. Soulopoulos; A. M. K. P. Taylor and Y. Urata. Schlieren-based temperature measurement inside the cylinder of an optical spark ignition and homogeneous charge compression ignition engine, *Appl. Opt,* **2015** ,*54 (14),* 4566-4579. https://doi.org/10.1364/AO.54.004566
23. H. Schardin. Schlieren methods and their applications, Ergebnisse der Exakten Naturwissenschaften 20 303–439 (1942).

24. R.A. Burton. A modified schlieren apparatus for large areas of field, *JOSA,* **1949** , *39(11),* 907-908. https://doi.org/10.1364/JOSA.39.000907
25. R.A. Burton. Notes on the multiple source Schlieren system, *JOSA,* ***1951*** ,41, 858–859. https://doi.org/10.1364/JOSA.41.000858
26. R.W. Fish and K. Parham. Focusing schlieren systems, British Aeronautical Research Council, Report CP-54 (1950).
27. A. Kantrowitz and R. L. Trimpi. A sharp-focusing schlieren system, *J. Aeronaut. Sci.,* **1950** , *17*, 311-314. https://doi.org/10.2514/8.1623
28. L. Weinstein. Review and update of lens and grid schlieren and motion camera schlieren, *Eur. Phys. J.-Spec. Top.* **2010** ,*182*, 65–95. https://doi.org/10.1140/epjst/e2010-01226-y
29. L.M. Weinstein. Large-field high-brightness focusing schlieren system, *AIAA J.* **1993** ,*31*, 1250–1255. https://doi.org/10.2514/3.11760
30. K. A. Ahmed. A. Wiley, Structured light-field focusing for flowfield diagnostics, *Exp. Therm. Fluid Sci.* **2017** ,*89*, 110–118. https://doi.org/10.1016/j.expthermflusci.2017.08.003
31. T. Kouchi; C.P. Goyne; R.D. Rockwell and J.C. McDaniel. Focusing-schlieren visualization in a dual-mode scramjet, *Exp. Fluid.* **2015** ,*56*, 211. https://doi.org/10.1007/s00348-015-2081-9
32. Drew L'Esperance and Benjamin D. Buckner. Focusing schlieren systems using digitally projected grid, Applied Optical Metrology II, edited by Erik Novak, James D. Trolinger, Proc. of SPIE Vol. 10373, 103730R
33. X. Jiang; Q. Cheng; Z. Xu; M. Qian and Q. Han. Quantitative measurement of acoustic pressure in the focal zone of acoustic lens-line focusing using the Schlieren method, *Appl. Opt.* **2016** ,*55 (10),* 2478-2483, https://doi.org/10.1364/AO.55.002478.
34. O. N. Stavroudis. The Optics of Rays, Wavefronts, and Caustics, Academic Press, Inc., (1972)
35. R. J. Goldstein and T. H. Kuehn. Optical systems for flow measurement: shadowgraph, Schlieren, and interferometric techniques, in Fluid Mechanics Measurements, R. J.Goldstein, ed., Taylor & Francis, London, (1996).
36. E. Hecht. Optics, Addison-Wesely Publishing Co., Inc., (2001).
37. C. Shakher; A. J. P. Daniel and A. K. Nirala. Temperature profile measurement of axisymmetric gaseous flames using speckle photography, speckle shearing interferometry, and Talbot interferometry, *Opt. Eng.* **1994** ,*33*, 1983–8. https://doi.org/10.1117/12.168849